

Feasibility Study of X-ray Fluorescence Imaging System: Surface Modification Gold Nanoparticles and 2D Convolutional Neural Network

Taeyun Kim ^{a,c}, Wooseung Lee ^a, Jimin Lee ^a, Sung-Joon Ye ^{a,b*}

^aProgram in Biomedical Radiation Sciences, Department of Transdisciplinary Studies, Graduate School of Convergence Science and Technology, Seoul National University, 08826, Seoul, Republic of Korea

^bAdvanced Institutes of Convergence Technology, Seoul National University, 16229, Suwon, Republic of Korea
^cNeutron and Radioisotope Application Research Division, Korea Atomic Energy Research Institute, 34057, Daejeon, Republic of Korea

*Corresponding author: sye@snu.ac.kr

1. Introduction

Recently, researches on tumor diagnosis and radiation therapy using metal nanoparticles (MNPs) (e.g., gadolinium, platinum, silver, and gold) have been actively conducted. Among them, gold nanoparticles (GNPs) have been most extensively studied. Because gold is an inert metal, its biocompatibility is superior to other MNPs. Moreover, various types of surface modifications (e.g., poly(ethylene) glycol, antibody, and protein) can be used to improve tumor-targeting ability (e.g., enhanced permeability and retention (EPR) effect). After GNPs accumulated in the tumor region, they can serve as the imaging contrast agents and radiosensitizers due to the high X-ray absorption coefficient derived from a high-atomic number [1].

When conducting *in vivo* imaging and therapeutic studies with MNPs, it is very important to evaluate the biological effects. For a more accurate evaluation, it is essential to obtain the *in vivo* biodistribution of MNPs. X-ray fluorescence computed tomography (XFCT) and X-ray fluorescence (XRF) imaging based on X-ray fluorescence (i.e., Characteristic X-ray) are emerging as promising *in vivo* imaging modalities that can obtain the *in vivo* biodistribution of MNPs (i.e., XRF image) [2, 3].

In 2019, a benchtop XFCT system with a linear array cadmium zinc telluride (CZT) detector and a single pinhole collimator was developed for *in vivo* imaging of the gadolinium nanoparticles in living mice [2]. This benchtop XFCT system required an XRF image acquisition time of 7.5 min per target slice. More recently, our previous study reported an XRF imaging system with a commercial 2D CZT gamma camera and a single pinhole collimator for dynamic *in vivo* imaging of the GNPs in living mice [3]. With the implementation of a 2D CZT gamma camera, the XRF image acquisition time was reduced to 2 min per target slice.

The aforementioned XFCT and XRF imaging systems have limitations in common with the advantages and disadvantages that are offset by each other. In the case of the XRF imaging system, the dynamic *in vivo* XRF images could be obtained due to dramatically shorter image acquisition time than the XFCT system. Whereas, the XRF imaging system has a limitation that essentially requires an XRF image before the injection of MNPs (i.e., pre-scanning) for the direct subtraction method (i.e., Compton background elimination), unlike the XFCT system. This can generate artifacts by position error and

double the imaging dose and image acquisition time. In addition, both systems investigated the feasibility of *in vivo* XRF image acquisition using pure MNPs without surface modification.

In this study, we investigated the feasibility of XRF imaging system with surface modification GNPs and 2D convolutional neural network (CNN) for Compton background elimination. The *in vivo* XRF image obtained by injecting liposomal GNPs into tumor-bearing mice was used to investigate the tumor-targeting ability improvement of liposomal GNPs. Furthermore, for substituting pre-scanning XRF image acquisition, which was the major limitation of our previous XRF imaging system, Compton background elimination was performed using pre-developed 2D CNN.

2. Methods and Results

2.1 Mice study

A mice study was conducted with our previous XRF imaging system (Fig. 1.) [3].

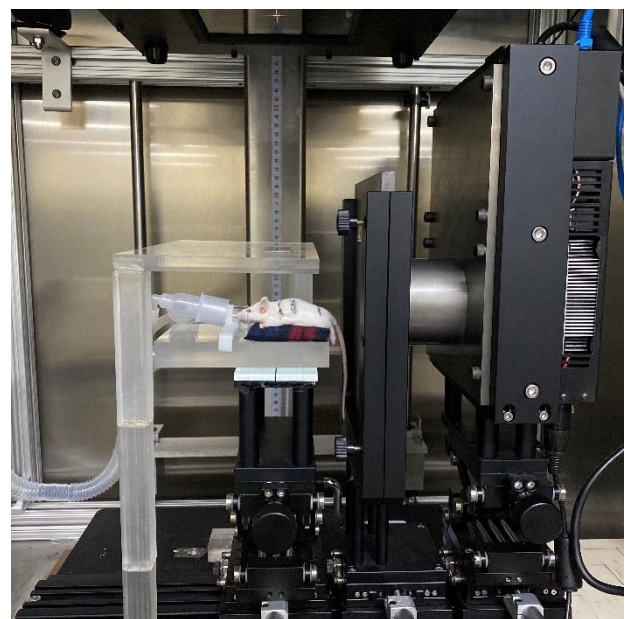


Fig. 1. XRF imaging system with a commercial 2D CZT gamma camera and a single pinhole collimator.

Three 4T1 tumor-bearing Balb/C mice were used. Mice were anesthetized with isoflurane gas via inhalation. 12

mg of liposomal GNPs were suspended in 100 μ L phosphate-buffered saline solution then injected through the tail vein. The target slice was 4T1 tumor slice and scanned with a 2 mm thickness fan-beam X-ray.

Unlike our previous XRF imaging study, the scanning procedure was only a post-scanning procedure after liposomal GNPs injection. Post-scanning was performed for 1 min at T=0 (i.e., immediately after injection), 4, and 24 hours. This is because mice were left freely after every time point scanning. It means that pre-scanning XRF image before GNPs injection cannot be obtained and the direct subtraction method for Compton background elimination cannot be performed.

Fig. 2 shows the different prone position of the mouse at T=24 hours. When XRF images were obtained at the straight prone position, the tumor region was located outside the 2D CZT gamma camera field of view (FOV). To locate the tumor region inside the FOV, the position of the mice was changed from a straight prone position to a curved prone position.



Fig. 2. (a) Photograph of the straight prone position of mouse. (b) Photograph of the curved prone position of mouse. The red circle indicates a 4T1 tumor.

2.2 2D CNN model

2D CNN model was trained using XRF images obtained from an imaging phantom with GNP columns of which concentrations were 0, 0.125, 0.25, 0.5, 1.0, and 2.0% by gold weight (wt%). The model was pre-developed for a preliminary study and applied for this mice study as well.

2.3 Experimental result

Fig. 3 and 4 show the XRF images at post-injection T=24 hours with the straight and curved prone position. The top row shows XRF images with Compton background and the bottom row shows XRF images without Compton background. Compton background elimination was successfully performed using 2D CNN. As mentioned in section 2.1, when the position of mice was the straight prone position, the tumor region could not be confirmed in XRF images.

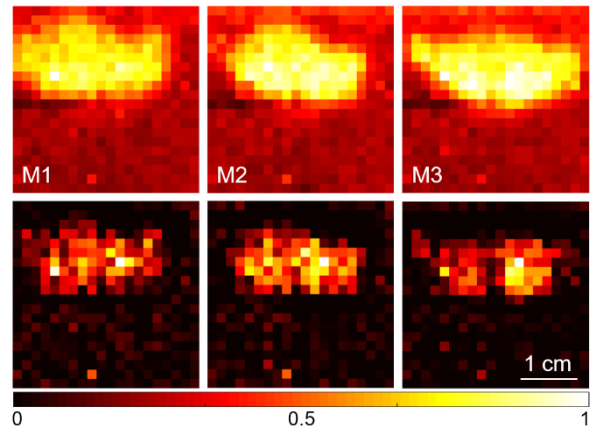


Fig. 3. XRF images at post-injection T=24 hours with the straight prone position. The color bar depicts the XRF signal (a.u., arbitrary units).

When XRF images were obtained at a curved prone position, the tumor region is located inside the FOV of the 2D CZT gamma camera. In particular, as shown in the bottom row of Fig. 4, it seems that the liposomal GNPs were sufficiently accumulated in the tumor region. However, it is not reasonable to evaluate the tumor-targeting ability of liposomal GNPs with only these XRF images.

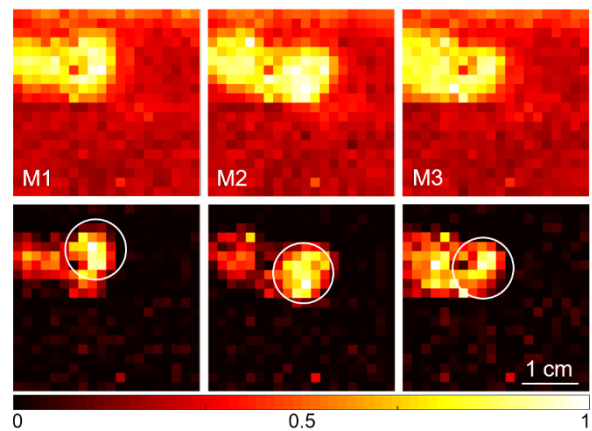


Fig. 4. XRF images at post-injection T=24 hours with the curved prone position. The white circles indicate a tumor region. The color bar depicts the XRF signal (a.u., arbitrary units).

3. Conclusions

A feasibility study of XRF imaging system with surface modification GNPs and 2D CNN was investigated. The pre-developed 2D CNN has been successfully validated, to substitute the indispensable pre-scanning XRF image of our previous XRF imaging study. Applying the 2D CNN to eliminate Compton background, artifacts due to position errors can be reduced, and imaging dose and image acquisition time can be reduced in half compared to our previous XRF imaging study.

In addition, investigated the tumor-targeting ability

improvement of liposomal GNPs. As mentioned in section 2.3, it is essential to verify whether liposomal GNPs accumulated in the tumor using a validated *ex vivo* analysis method (e.g., ICP-AES, ICP-MS, and L-shell XRF detection system) to validate the tumor-targeting ability improvement of liposomal GNPs. In addition, liposomal GNPs and pure GNPs (i.e., control group) inject into living mice of the same conditions then need to compare the difference of GNPs accumulation in the tumor.

REFERENCES

- [1] S. Her, DA. Jaffray, and C. Allen, Gold nanoparticles for applications in cancer radiotherapy: Mechanisms and recent advancements, *Adv Drug Deliv Rev*, Vol. 109, p. 84-101, 2017.
- [2] S. Zhang, L. Li, J. Chen, Z. Chen, W. Zhang, and H. Lu, Quantitative imaging of Gd nanoparticles in mice using benchtop cone-beam x-ray fluorescence computed tomography system, *Int J Mol Sci*, Vol. 20, p. 2315-2327, 2019.
- [3] S. Jung, T. Kim, W. Lee, H. Kim, H. S. Kim, H. J. Im and S. J. Ye, Dynamic in vivo x-ray fluorescence imaging of gold in living mice exposed to gold nanoparticles, *IEEE Trans Med Imaging*, Vol. 39, p. 526-533, 2020.